POLITECNICO DI TORINO
Repository ISTITUZIONALE

Conceptual design of a SuperConducting Energy Pipeline for LH2 and power transmission over long distances

Original
Conceptual design of a SuperConducting Energy Pipeline for LH2 and power transmission over long distances / Savoldi, Laura; Balbo, Alessandro; Bruzek, Christian E.; Grasso, Gianni; Patti, Matteo; Tropeano, Matteo. - In: IEEE TRANSACTIONS ON APPLIED SUPERCONDUCTIVITY. - ISSN 1051-8223. - (2024), pp. 1-5. [10.1109/tasc.2024.3370123]

Availability:
This version is available at: 11583/2987318 since: 2024-03-26T14:19:47Z

Publisher:
IEEE

Published
DOI:10.1109/tasc.2024.3370123

Terms of use:

This article is made available under terms and conditions as specified in the corresponding bibliographic description in the repository

Publisher copyright

(Article begins on next page)

17 June 2024

This article has been accepted for publication in IEEE Transactions on Applied Superconductivity. This is the author's version which has not been fully edited and content may change prior to final publication. Citation information: DOI 10.1109/TASC.2024.3370123

4-LS-SS-03S

Conceptual design of a SuperConducting Energy Pipeline for LH_2 and power transmission over long distances

Laura Savoldi, *Member, IEEE*, Alessandro Balbo, Christian E. Bruzek, Gianni Grasso, Matteo Patti and Matteo Tropeano

***Abstract*—The design of a single-pole MgB_2 superconducting hydrogen-cooled cable for DC current transmission at low voltage (10 kV) is presented here. The cable consists of a former made of MgB_2 superconducting wires, a dielectric layer and an annular region that allows for the passage of hydrogen at inlet pressures above the critical one. The cable is contained within a corrugated cryostat, insulated from the external environment. The use of MgB_2 as a superconducting material allows for the operation of the cable in the range 15-27 K, which reduces the cooling requirements and increases the efficiency of the system. The hydrogen-cooled annular region, acting as a pipeline for the cryogen transport, allows at the same time the efficient cooling of the cable, while the corrugated cryostat provides additional insulation and structural support, together with a relief volume in the case of an accident. The results of this study, mainly performed with a simplified model, benchmarked against the OPENSC^2 software, show that the cable is able to support DC current transmission at 10 kV, with maximum cable lengths of several tens of km for inner diameters of the cryostat > 120 mm, supporting a H_2 mass flow rate > 1 kg/s. Overall, this study demonstrates the feasibility of combining the DC current transmission at low-medium voltage by MgB_2 to the transport of liquid hydrogen, providing at the same time instantaneous storage of chemical power.**

***Index Terms*— Power cables, hydrogen economy, MgB_2 wires and tapes, energy storage.**

I. INTRODUCTION AND CONTEXT

THE combined transfer of electricity and liquid hydrogen LH_2 in a SuperConducting Energy Pipeline (SCEP) is a 20-years old idea. P. Grant pioneered the idea of a "Energy Super-Cable", simultaneously transmitting chemical and electric power over long distances in [1], [2]. The 1 GW electric power transfer (100 kA at $\pm$5kV) was assumed to be based on a MgB_2 superconducting line, while the chemical power transfer was designed by considering liquid hydrogen as the cryogen to cool the SC cable, or by a secondary flow of gaseous hydrogen or methane, in the case the cable cooling is provided by liquid nitrogen. Although the layout of the cable was not specified, and only the diameter of the LH_2 channel was discussed, a dimensionless figure of merit to determine the relative transport of electric and chemical power was proposed, that can be useful to define an efficiency of the pipeline. A hybrid MgB_2/LH_2 20-km long pipeline was studied in [3] for the exploitation of large-scale renewable energy systems, with particular reference to the identification of the most suitable operating range for the LH_2, with temperature in the range 15-25 K and pressure 0.5 – 1.5 MPa. In [4], [5] a 1 GW hybrid energy transfer line of 1000 km was addressed with hydrogen made from the steam electrolysis, where the heat is obtained from the waste heat of a nuclear fusion device on site. The electric power is transferred using a MgB_2 DC power line at 10 kA and 100 kV, with a liquid hydrogen mass flow rate of 100 tons per day at 0.4 MPa. The operating temperature is 17 -24 K, assuming the presence of refrigeration stations every 10 km of the unit section. A low-voltage DC SCEP is described in [6] as a key component of micro-power grid systems to balance power demand and supply, or for stand-alone applications. More recently, a HTS energy pipeline integrating an electric power cable with LH_2 and liquefied natural gas (LNG) has been investigated in [7], and demonstrated to be economically and technically viable to be inserted into a gas-insulated metal

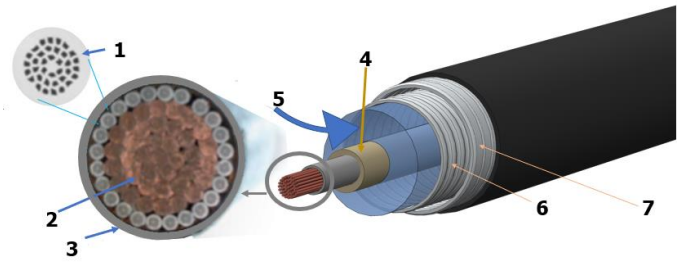

Fig. 1. Reference layout for the SCEP addressed in this study: 1. MgB2 strand; 2. Copper strands; 3. Stainless-steel wrapping; 4. Cold dielectric; 5. LH2 flow; 6. Inner cryostat, with thermal insulation (not shown); 7. Outer cryostat, with a polyethylene external layer (in black in the sketch).

Laura Savoldi and Alessandro Balbo are with Dipartimento Energia "Galileo Ferraris", Politecnico di Torino, Torino, I-10129 Italy (e-mail:laura.savoldi@polito.it, alessandro_balbo@polito.it).

Christian E. Bruzek, Gianni Grasso and Matteo Tropeano are with ASG Superconductors, Genoa, I-16152 Italy (grasso.gianni@as-g.it, bruzek.christian-eric@as-g.it, tropeano.matteo@as-g.it)

Matteo Patti was with Dipartimento Energia "Galileo Ferraris", Politecnico di Torino, Torino, I-10129 Italy.

Color versions of one or more of the figures in this article are available online at http://ieeexplore.ieee.org

This work is licensed under a Creative Commons Attribution-NonCommercial-NoDerivatives 4.0 License. For more information, see https://creativecommons.org/licenses/by-nc-nd/4.0/

This article has been accepted for publication in IEEE Transactions on Applied Superconductivity. This is the author's version which has not been fully edited and content may change prior to final publication. Citation information: DOI 10.1109/TASC.2024.3370123

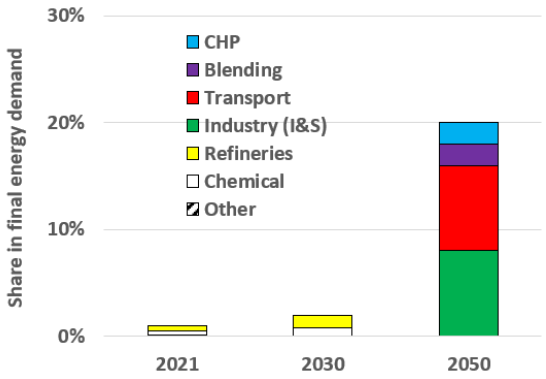

Fig. 2. Increase in the Hydrogen share in final energy demand foreseen in the Preliminary Guidelines of the Italian National Hydrogen Strategy [13], split by end-use.

enclosed transmission line [8].

The "hydricity" (combination of "hydrogen" and "electricity") concept embedded in the SCEP is also moving from paper to real world. The first 10-m-long experimental proof-of-concept was successfully manufactured with MgB_2 and tested in Russia in 2011 [9]. In 2013, a second 30-m-long prototype proved the feasibility of operating a 2-kA cable cooled by LH_2 within 20–26 K, pressures in the interval from 0.15 to 0.5 MPa, and mass flow rates up to 250 g/s [10], [11]. A 10-m-long hybrid pipeline with Bi2223 tapes was also successfully tested in China, as reported in [12]. The successful tests of SCEPs could become a turning point in a political context with a significantly increasing demand for electrification and substitution of fossil fuels with hydrogen.

The Italian National Hydrogen Strategy (Preliminary guidelines) [13], issued by the former Ministry of Economic Development, is taken here as an example of the vision and targets for hydrogen penetration "toward a decarbonized and sustainable economy", as reported in Fig. 2. By 2030, the ambition is to reach a 2% hydrogen penetration in final energy demand, including applications in long-distance freight transport [14], heavy industry, refineries and blending into the gas grid, starting from a penetration of 1% in 2021. By 2050, the target increases up to 20% (including also aviation, see e.g. the studies in [15], [16], energy storage in the power sector [6] and residential buildings applications). The largest fraction of that amount of hydrogen is expected to be supplied by electrolysers, according to [17]. However, they currently represent the most expensive hydrogen production alternative, albeit representing a zero-emissions technology whenever electricity from clean sources is used. The strategy defines three theoretical models of green hydrogen production: complete on-site production (linked also to the hydrogen valleys, industrial clusters of concentrated production and consumption), on-site production with renewable electricity transportation and centralized production with hydrogen transportation. It is already established that the most efficient way of transferring hydrogen is in its liquid form, i.e., in cryogenic conditions, as that maximize the energy transfer rate minimizing the dimension of the pipeline, so that the transfer of hydrogen matches the transfer of electric power via superconductors.

The aim of this paper is to carry out the conceptual design of a DC single-pole single-coolant 0.1 GWe, > 0.1 GWt and GJ-class (0.1-1 GWh-class) storage SCEP. The targeted electric power, achieved with a cable at nominal current of 10 kA at a medium voltage of 10 kV, mimics that already demonstrated in the BEST PATHS European project [18]. The target on the thermal (chemical) power can be evaluated for the caloric value CV of the hydrogen transferred by the pipeline, while the stored energy, proportional to the hydrogen mass in the pipeline, comes as a fringe benefit. Note that the target power is here much less than other projects of the same type currently running in Europe, such as the Flagship Project TransHyDE one in Germany with 4 GW_e and 0.87 GW_t [19] and Horizon Europe project SCARLET, investigating systems that will deliver 1-2 GWe and nearly up to 0.5 GWt [20]. The reason behind this choice, beside taking advantage of already developed SC cables, is that it could be preferable to reach a large power transfer by means of multiple "small" SCEPs in parallel rather than with a single pipeline, for the sake of maintainability, redundancy and security of the supply.

II. Methodology for the SCEP Design

A. Design by functional analysis

The preconceptual design of the SCEP has been performed according to a functional analysis process, which allows translating the system-level requirements into detailed functional and performance requirements for the sub-components, see for instance [21]. The process functions, dealing directly with the operation of the SCEP at the target operating parameters, are to guarantee that the device carries the rated current at the rated voltage and to guarantee that the device transfers the rated chemical energy. When one progressively splits the top-level functions into lower level ones, almost automatically achieves the main features that the design of the sub-components (the SC cable, the cooling duct, the terminations, …) should fulfill, allowing to easily achieve the preconceptual design. Moreover, this technique allows an easy identification of the fault conditions [22], defined by an imperfect fulfillment of the different process functions, and the identification of appropriate sub-components fulfilling the functions to "protect the investment".

The resulting SCEP layout is sketched in Fig. 2. It has concentric structure, with the SC cable in the middle, surrounded by the cold dielectric. This is inserted into the LH_2 channel, confined by a corrugated pipe that constitutes the inner side of the cryostat. A vacuum chamber is present between the inner cryostat at cryogenic temperature and the outer cryostat at room temperature. The two cryostats are kept apart by a low-conduction spacer, to limit the thermal transfer between them. To limit radiation heating, the inner cryostat is additionally lapped with super-insulation (MLI). A polyethylene layer is present on the outer surface of the outer cryostat, for mechanical and chemical protection and to help in the pipeline installation. Note that this simple design does not consider possible alternative solutions to reduce the parasitic load, such as

This work is licensed under a Creative Commons Attribution-NonCommercial-NoDerivatives 4.0 License. For more information, see https://creativecommons.org/licenses/by-nc-nd/4.0/

This article has been accepted for publication in IEEE Transactions on Applied Superconductivity. This is the author's version which has not been fully edited and content may change prior to final publication. Citation information: DOI 10.1109/TASC.2024.3370123

evaporative conditions for the cryogen [23], or double cooling channels to increase the thermal shielding of the cable [24].

B. SC cable design

For an operative current I_{op} = 10 kA, the development of MgB_2 strands and cable performed for the BEST PATHS project can be fully deployed, where the cable has been already produced with an industrial cabling machine [24]. The cable is assembled using a core with 37 Cu strands, surrounded by 24 MgB_2 strands with a diameter of 1.33 mm. Each strand is a Monel/Nickel sheathed round wire containing 36 MgB_2 filaments, with a Cu/NonCu ratio of 1.54. The measured critical current for the strands guarantees that the cable is capable to carry the rated current up to 27 K, with still a 25% margin to current sharing. The resulting cable, having a linear density ≤ 1 kg/m, is shown in the inset in Fig. 1, wrapped by a 0.5-mm stainless steel tape with some gap between the tapes, to withstand the pressure from the lapping of the dielectric insulation. The diameter of the cable at this stage is $d_i \sim 12$ mm. As far as the dielectric is concerned, its sizing has been performed following (1), that applies to standard cylindrical configurations [25]:

$$d_o = d_i \times e^{\frac{V}{d_i/2 \times SF \times E_b}} \sim 15 \text{ mm} \qquad (1)$$

In (1), d_o is the outer diameter of the cylinder, V is the rated voltage (10 kV in this case), the breakdown voltage $E_b = 20 \frac{\text{kV}}{\text{mm}}$ for a 10-kV class cable, reduced by an appropriate safety factor $SF \sim 0.3$. Note that, although the dielectric properties of LH_2 are not well-known yet, (1) has already been used for LH_2/paper insulation subject to dc operation in [25].

C. Cooling channel sizing

For the design of the cooling duct (see Fig. 1), the pressure-enthalpy diagram for the subcooled para-hydrogen (reported in Fig. 3) was carefully analyzed. Also based on work done by other scholars, 3 different conditions for the inlet pressure p_{in} have been considered, and namely 2 MPa, 3 MPa and 4 MPa, with a corresponding inlet temperature T_{in} of 15 K in the former case and 16 K (to avoid solidification) in the others. In view of the critical current of the MgB_2 cable, an outlet temperature $T_{out} \leq 27$ K, has been retained for the analysis. To allow for a parametric investigation of the possible relevant operating conditions, three different thermal levels were considered at the SCEP outlet, and namely 21 K, 24 K and 27 K, imposing an outlet pressure p_{out} ~1 bar larger than the corresponding saturation pressure at T_{out}. Note that this condition could be easily realizable by connecting the pipeline outlet to a tank with saturated H_2 at the desired saturation temperature by means of a valve with a controlled pressure head. Among the different possible desired trajectories for the LH_2 in Fig. 3, the ones with a large pressure drop could be favorable to transfer large LH_2 flow rates, while the ones with a large enthalpy increase could be favorable to bear the parasitic heat load along long lengths.

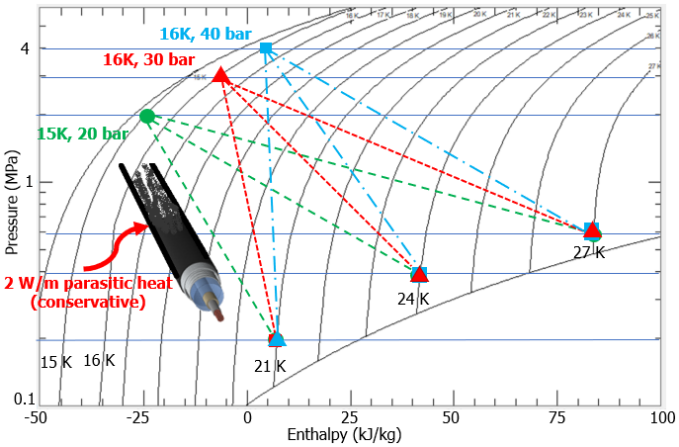

Fig. 3. Pressure-enthalpy ($\boldsymbol{p}, \boldsymbol{h}$) diagram for the subcooled para-hydrogen, obtained using the MiniREFPROP library by NIST, with highlighted the wished trajectories of the LH_2 along the SCEP.

The function of cryogen flow containment is fulfilled using a corrugate pipe (see Fig. 1). Commercial pipes with different Inner/Outer diameter (ID/OD) were retained as possible candidates for the inner cryostat, confining the flow, as shown in Table I. For all pipes, it must be ensured that the wall is sufficiently thick to withstand the highest pressure it may experience (p_{in}), evaluated according to the standard ASME standards for process piping [26]. At the same time, the wall thickness should not exceed the maximum value of ~1 mm, which sets the constraint on the allowed p_{in} for the different diameters. Note that in all cases the linear density of the pipe is $\sim 1 - 5$ kg/m, depending on the size.

TABLE I
THICKNESS (mm) OF THE CORRUGATED PIPE TO WITHSTAND DIFFERENT LH_2 INLET PRESSURE

ID/OD (mm)	p_{in} = 2 MPa	p_{in} = 3 MPa	p_{in} = 4 MPa
39/44	0.21	0.31	0.42
60/66	0.31	0.47	0.62
76/85	0.40	0.60	0.80
100/110	0.52	0.78	1.04
127/143	0.71	1.06	>1.1
147/163	0.77	>1.1	>1.1
198/220	1.04	>1.1	>1.1

In the evaluation of the pressure drop along the pipes, as a first approximation the corrugation can be considered as a surface roughness, which is evaluated according to (2), where ε is the relative roughness.

$$\varepsilon = \frac{OD - ID}{OD + ID} \qquad (2)$$

For all the commercial corrugate pipes considered here, ε does not exceed 5-6%, allowing estimating conservatively the friction factor $f = 0.08$ independently on the mass flow rate in the turbulent regime, according to the Moody diagram [27] (not shown). Note that for all the corrugate pipes considered here, the presence of the SC cable within the pipeline has been considered just by properly reducing the flow area A and increasing the wetted perimeter of the duct P_{wetted} as in (3-4), while any friction related to flow boundary layer developing along the SC cable has been ignored. Note, however, that d_o results to be significantly

This work is licensed under a Creative Commons Attribution-NonCommercial-NoDerivatives 4.0 License. For more information, see https://creativecommons.org/licenses/by-nc-nd/4.0/

This article has been accepted for publication in IEEE Transactions on Applied Superconductivity. This is the author's version which has not been fully edited and content may change prior to final publication. Citation information: DOI 10.1109/TASC.2024.3370123

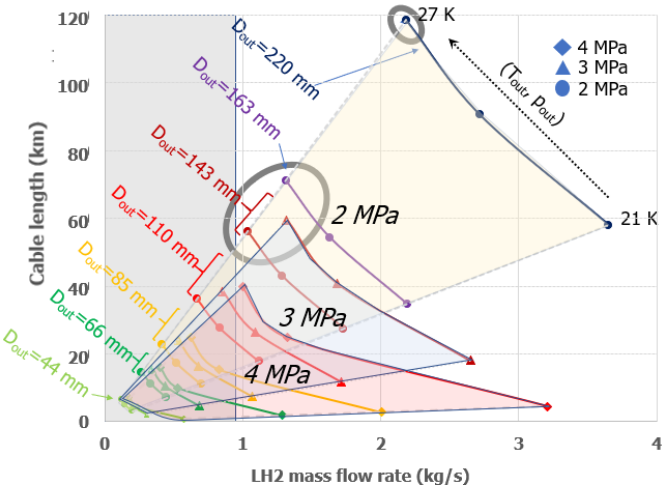

Fig. 4. SCEP $\dot{m}$ and length L resulting for the different trajectories (diamonds with red-shaded area for p_{in}= 4 MPa, triangles with blue-shaded area for p_{in}= 3 MPa and circles with yellow-shaded area for p_{in}= 2 MPa, respectively), for the different corrugate pipeline size considered in this study. The grey area indicates the solutions below the rated thermal power target.

smaller than the diameter of the selected cooling ducts, so that A and P_{wetted} are only marginally affected by the SC cable.

$$A = \frac{\pi}{4}\left[\left(\frac{OD+ID}{2}\right)^2 - (d_o)^2\right] \quad (3)$$

$$P_{wetted} = \pi\left(\frac{OD+ID}{2} + d_o\right) \quad (4)$$

To estimate the LH_2 mass flow rate $\dot{m}$ and SCEP length L, steady-state momentum and energy balance equations were written as in (5-6), considering the fluid as incompressible with the density ρ evaluated at the average pressure and temperature of the different possible trajectories in Fig. 3.

$$\Delta p = p_{in} - p_{out} = \frac{f}{8\rho A^3} L P_{wetted} \dot{m} \quad (5)$$

$$\dot{q}L = \dot{m}(h_{out} - h_{in}) \quad (6)$$

For all trajectories and all possible corrugate diameter, the parasitic load per unit length $\dot{q}$ is set to 2 W/m, whereas it has been demonstrated that this value could be cut by a factor of 10 in the case of proper thermal shielding [28]. Note that the parasitic load depends on the considered diameter, but the selected value is conservative for all diameters considered in this study.

The set (5-6) allows computing directly the two unknowns, and namely the couple $(\dot{m}, L)$ for the set of trajectories highlighted in Fig. 3 and for all the corrugate pipe diameters. The incompressibility assumption for the case at end was assessed by the comparison obtained using the OPENSC$_2$ code [29], and shown to impact only marginally the broad picture of the results.

III. Resulting SCEP Design

The result of the LH_2 duct sizing is reported in Fig. 4, where the colored-shaded areas identify the trajectories beginning with the cryogen at the different values of p_{in}. It is clearly visible that the increase in the corrugate diameter allows for larger $\dot{m}$ and longer pipelines at all values of p_{in}, along all possible trajectories, as expected. Higher temperature (and pressure) at the outlet of the pipeline allows to reach longer pipelines (the allowed enthalpy increase is higher) but smaller values of $\dot{m}$ (the allowed pressure drop is smaller) than in the case of T_{out} = 21 K.

For any given corrugate diameter, p_{in} affects the LH_2 $\dot{m}$, with a very limited impact on the cable length. A smaller p_{in} allows for longer pipeline lengths and higher values of $\dot{m}$, since larger corrugate pipes can be used (see Table I). Only if one sticks to a pipeline with OD ≥143 mm, p_{in} = 2 – 3 MPa and T_{out} set at the maximum value of 27 K, the pipelines along the two possible trajectories (in the grey circles in Fig. 4) reach a length > 50 km, transferring a mass flow rate $\dot{m}$ > 1 kg/s. Such a LH_2 flow delivers a thermal (chemical) power evaluated in (7) (where CV = 33.33 kWh/kg) that is always above the target of 0.1 GWt.

$$Q_t = \dot{m} \times CV \quad (6)$$

The energy stored in the pipeline E_{LH_2} can be evaluated from CV and the mass per unit length m', considering the different pipeline lengths as in Table II. All the pipelines designed along the trajectories compliant with the Q_t target store an energy in the 1-10 GWh class, one order of magnitude higher than what was wished.

TABLE II

Features of the designed SCEP with p_{in} = 2 MPa

OD	A	$\dot{m}$	m'	L	E_{LH_2}
(mm)	(cm^2)	(kg/s)	(kg/m)	(km)	(MWh/km)
143	140	1.0	1.0	55	>30
163	190	1.3	1.3	70	>40
220	340	2.2	2.4	115	~80

III. Discussion and Perspective

A methodology for the design of a DC single-pole single-coolant SuperConducting Energy Pipeline, transferring in nominal conditions an electric power of 0.1 GW$_e$, and a thermal (chemical) power >0.1 GW$_t$ with a cryogenic LH_2 flow has been developed by functional analysis. Different possible configurations have been found, all based on the BEST PATHS MgB_2 cable, investigating different corrugate duct diameters along different pressure-temperature trajectories. Although some specific aspects, such as the dielectric properties of LH_2, still need to be clarified experimentally, under the conservative parasitic load of 2 W/m, lengths above 50 km can be reached with a corrugate OD ≥ 143 mm, p_{in} ~ 2-3 MPa and T_{out} reaching 27 K.

As next steps, the conceptual design of the active auxiliaries, such as current leads and cryogenic pumps, will be carried out, together with a preliminary thermo-mechanical assessment and the analysis of effects of fault conditions. All that will allow the assessment of the techno-economic competitiveness of the possible alternative configurations with respect to different technologies for the separate transfer of power and H_2. The techno-economic assessment of the SCEP will also allow to insert the two joint commodities electricity and hydrogen in energy system optimization models such as the TEMOA-Italy [30], to evaluate what is the minimum cost of the SCEP technology that could allow the profitable adoption of such technology in the Italian reference energy system.

This work is licensed under a Creative Commons Attribution-NonCommercial-NoDerivatives 4.0 License. For more information, see https://creativecommons.org/licenses/by-nc-nd/4.0/

This article has been accepted for publication in IEEE Transactions on Applied Superconductivity. This is the author's version which has not been fully edited and content may change prior to final publication. Citation information: DOI 10.1109/TASC.2024.3370123

ACKNOWLEDGMENT

The authors would like to thank Dr. D. Lerede, Mr. S. Palacios and Prof. L. Rossi for very useful discussion.

REFERENCES

[1] P. M. Grant, "The SuperCable: Dual delivery of chemical and electric power," *IEEE Trans. Appl. Supercond.*, vol. 15, no. 2 PART II, pp. 1810–1813, Jun. 2005, doi: 10.1109/TASC.2005.849298.

[2] P. M. Grant, "Could SuperCables deliver both hydrogen and electricity via a SuperGrid?," *Power*, vol. 151, no. 5, May 2007.

[3] L. Trevisani, M. Fabbri, and F. Negrini, "Long distance renewable-energy-sources power transmission using hydrogen-cooled MgB2 superconducting line," *Cryogenics (Guildf).*, vol. 47, no. 2, pp. 113–120, Feb. 2007, doi: 10.1016/J.CRYOGENICS.2006.10.002.

[4] S. Yamada, Y. Hishinuma, T. Uede, K. Schippl, and O. Motojima, "Study on 1 GW class hybrid energy transfer line of hydrogen and electricity," *J. Phys. Conf. Ser.*, vol. 97, no. 1, p. 012167, Feb. 2008, doi: 10.1088/1742-6596/97/1/012167.

[5] S. Yamada *et al.*, "Conceptual design of 1 GW class hybrid energy transfer line of hydrogen and electricity," *J. Phys. Conf. Ser.*, vol. 234, no. 3, p. 032064, Jun. 2010, doi: 10.1088/1742-6596/234/3/032064.

[6] T. Nakayama, T. Yagai, M. Tsuda, and T. Hamajima, "Micro power grid system with SMES and superconducting cable modules cooled by liquid hydrogen," *IEEE Trans. Appl. Supercond.*, vol. 19, no. 3, pp. 2062–2065, Jun. 2009, doi: 10.1109/TASC.2009.2018743.

[7] J. Jin, L. Wang, R. Yang, T. Zhang, S. Mu, and Q. Zhou, "A composite superconducting energy pipeline and its characteristics," *Energy Reports*, vol. 8, pp. 2072–2084, Nov. 2022, doi: 10.1016/J.EGYR.2022.01.126.

[8] Z. Yu, Y. Ren, B. Cao, J. Liu, and Z. Zhou, "Feasibility and Economical Analysis of the Superconducting Cable and Hydrogen Hybrid Transmission Gallery," *2020 IEEE Int. Conf. Appl. Supercond. Electromagn. Devices, ASEMD 2020*, Oct. 2020, doi: 10.1109/ASEMD49065.2020.9276292.

[9] V. V. Kostyuk *et al.*, "Experimental hybrid power transmission line with liquid hydrogen and MgB2-based superconducting cable," *Tech. Phys. Lett. 2012 383*, vol. 38, no. 3, pp. 279–282, Apr. 2012, doi: 10.1134/S106378501203025X.

[10] V. S. Vysotsky *et al.*, "Hybrid energy transfer line with liquid hydrogen and superconducting MgB2 cable - First experimental proof of concept," *IEEE Trans. Appl. Supercond.*, vol. 23, no. 3, 2013, doi: 10.1109/TASC.2013.2238574.

[11] V. S. Vysotsky *et al.*, "Energy Transfer with Hydrogen and Superconductivity – The Review of the First Experimental Results," *Phys. Procedia*, vol. 65, pp. 299–302, Jan. 2015, doi: 10.1016/J.PHPRO.2015.05.158.

[12] J. Chen *et al.*, "Simulation and experiment on superconducting DC energy pipeline cooled by LNG," *Cryogenics (Guildf).*, vol. 112, p. 103128, Dec. 2020, doi: 10.1016/J.CRYOGENICS.2020.103128.

[13] Ministero dello Sviluppo Economico;, "Strategia Nazionale Idrogeno Linee Guida Preliminari," 2021.

[14] X. Chen, Z. Pang, M. Zhang, S. Jiang, J. Feng, and B. Shen, "Techno-economic study of a 100-MW-class multi-energy vehicle charging/refueling station: Using 100% renewable, liquid hydrogen, and superconductor technologies," *Energy Convers. Manag.*, vol. 276, p. 116463, Jan. 2023, doi: 10.1016/J.ENCONMAN.2022.116463.

[15] S. Telikapalli, R. M. Swain, P. Cheetham, C. H. Kim, and S. V. Pamidi, "Electric Aircraft Fueled by Liquid Hydrogen and Liquefied Natural Gas," *IOP Conf. Ser. Mater. Sci. Eng.*, vol. 1241, no. 1, p. 012035, May 2022, doi: 10.1088/1757-899X/1241/1/012035.

[16] C. Hartmann, J. K. Noland, R. Nilssen, and R. Mellerud, "Dual Use of Liquid Hydrogen in a Next-Generation PEMFC-Powered Regional Aircraft with Superconducting Propulsion," *IEEE Trans. Transp. Electrif.*, vol. 8, no. 4, pp. 4760–4778, Dec. 2022, doi: 10.1109/TTE.2022.3170827.

[17] Ministero dell'Ambiente e della Sicurezza Energetica, "PIANO NAZIONALE INTEGRATO PER L'ENERGIA E IL CLIMA," 2023.

[18] "Best Paths - Home." http://www.bestpaths-project.eu/ (accessed Sep. 17, 2023).

[19] S. Palacios, M. Wehr, M. J. Wolf, M. Noe, and T. Arndt, "Combined Energy transmission by LH2 and HTS: study of a hybrid pipeline." 2023.

[20] "Scarlet – Superconducting CAbles foR sustainabLe Energy Transition." https://scarlet-project.eu/ (accessed Sep. 25, 2023).

[21] S. Sparacio, A. Napolitano, L. Savoldi, S. Viarengo, and F. Laviano, "Design of a Module for a 10 MJ Toroidal YBCO Superconducting Magnetic Energy Storage," *IEEE Trans. Appl. Supercond.*, vol. 32, no. 4, Jun. 2022, doi: 10.1109/TASC.2022.3143085.

[22] M. Yazdani-Asrami, S. Seyyedbarzegar, A. Sadeghi, W. T. B. De Sousa, and D. Kottonau, "High temperature superconducting cables and their performance against short circuit faults: current development, challenges, solutions, and future trends," *Supercond. Sci. Technol.*, vol. 35, no. 8, p. 083002, Jul. 2022, doi: 10.1088/1361-6668/AC7AE2.

[23] V. P. Firsov, A. G. Galeev, V. V. Kostyuk, and I. V. Antyukhov, "Evaporating system for cryogenic support of long length HTS power cables," *Int. J. Hydrogen Energy*, vol. 43, no. 29, pp. 13594–13604, Jul. 2018, doi: 10.1016/J.IJHYDENE.2018.05.046.

[24] C. E. Bruzek *et al.*, "Cable Conductor Design for the High-Power MgB2 DC Superconducting Cable Project of BEST PATHS," *IEEE Trans. Appl. Supercond.*, vol. 27, no. 4, Jun. 2017, doi: 10.1109/TASC.2016.2641338.

[25] A. Morandi, "HTS dc transmission and distribution: concepts, applications and benefits," *Supercond. Sci. Technol.*, vol. 28, no. 12, p. 123001, Oct. 2015, doi: 10.1088/0953-2048/28/12/123001.

[26] "Process Piping ASME Code for Pressure Piping, B31," 2015, Accessed: Sep. 17, 2023. [Online]. Available: http://cstools.asme.org/.

[27] B. R. Munson, T. H. (Theodore H. Okiishi, W. W. Huebsch, and A. P. Rothmayer, "Fundamentals of fluid mechanics," p. 10, Accessed: Jun. 09, 2023. [Online]. Available: https://books.google.com/books/about/Fundamentals_of_Fluid_Mechanics.html?hl=it&id=R17cthBdckYC.

[28] Y. V. Ivanov *et al.*, "A proposal of the hybrid energy transfer pipe," *J. Phys. Conf. Ser.*, vol. 1857, no. 1, p. 012006, Apr. 2021, doi: 10.1088/1742-6596/1857/1/012006.

[29] L. Savoldi, D. Placido, and S. Viarengo, "Thermal-hydraulic analysis of SuperConducting cables for energy applications iwth a novel open object-oriented software: OPENSC2," *Cryogenics (Guildf).*, vol. 124, p. 103457, 2022.

[30] M. Nicoli, F. Gracceva, D. Lerede, and L. Savoldi, "Can We Rely on Open-Source Energy System Optimization Models? The TEMOA-Italy Case Study," *Energies*, vol. 15, no. 18, Sep. 2022, doi: 10.3390/EN15186505.

This work is licensed under a Creative Commons Attribution-NonCommercial-NoDerivatives 4.0 License. For more information, see https://creativecommons.org/licenses/by-nc-nd/4.0/